"Four-Dimensional" Protein Structures: Examples from Metalloproteins

MARCO FRAGAI, CLAUDIO LUCHINAT,* AND GIACOMO PARIGI

Centro Risonanze Magnetiche (CERM) and Department of Agricultural Biotechnology, University of Florence, Via Luigi Sacconi, 6, 50019 Sesto Fiorentino (Florence), Italy

Received March 15, 2006

ABSTRACT

The fact that an object, for example, a protein, possesses a three-dimensional structure seems an obvious concept. However, when the object is flexible, the concept is less obvious. Growing experimental data over several decades show that proteins are not rigid objects, but they may sample more or less wide ranges of different conformations. To stress this concept, we propose to call the range of sampled conformations the "fourth dimension" of the protein structure. Nuclear magnetic resonance is a precious technique to define this fourth dimension. Examples of conformational heterogeneity taken from the realm of metalloproteins and their functional implications are discussed.

Introduction

Elucidating the structure of a protein is necessary to understand its function. The three-dimensional X-ray structure of a protein provides a good description of the conformation occupying the global (or sometimes a local) energy minimum. However, it is more and more apparent that the function often depends upon higher energy conformations and, thus, upon protein mobility.[1−3] Indeed, in several cases, the existence of different conformations with similar energy has been demonstrated,[4−8] and sometimes these conformations correspond to different functional states.[9,10]

Solution structures determined by nuclear magnetic resonance (NMR) suffer from different drawbacks. A well-known "problem" in protein solution structure determination is that a poor definition in particular regions of a protein may occur, usually arising from the lack of experimental restraints. However, when not the result of poor experimental quality, the lack of restraints depends upon internal motions affecting these regions. The resulting structural family disorder may thus actually reflect an intrinsic conformational heterogeneity of the protein and should be seen as an additional piece of information rather than as a problem. The real structure, in this case, should be more appropriately represented by a family of conformations, each of them with its own population.

There is growing evidence that the width of the accessible conformational space can be very different from one protein to another, but it always has functional significance.[5,11] To stress its importance, we propose to call the width of the conformational space the *fourth structural dimension*. It will be minimal for well-folded proteins whose role does not depend upon structural changes, maximal for natively unfolded proteins whose physiological role may depend upon transiently adopting a variety of conformations, and intermediate for proteins with a well-defined three-dimensional structure but still undergoing important structural changes while performing their biological function.

In our definition of the fourth dimension, be it large or small, *there is no consideration of the time that it takes for the fourth dimension to be sampled by the protein*. However, this does not imply that the time scale of the associated motions is irrelevant, because it reflects the time scale of functional events. NMR is also an appropriate technique to estimate the time scale of motions, from seconds to picoseconds (Figure 1), and novel methods are continuously developed.[1,4,6,7,12−15] NMR can thus provide information both on conformational heterogeneity and on the time scale of the motions associated to it. As such, it can effectively complement X-rays in determining the four-dimensional structure of proteins.

Although the above considerations hold for all proteins, here, we focus on metalloproteins. Besides constituting the core research field of our lab, metalloproteins do provide a good variety of examples of different widths of the fourth structural dimension and its functional implications.

Variable Width of the Fourth Dimension

The energy landscape of a protein is a function of all its degrees of freedom, which are at least as many as the

* To whom correspondence should be addressed: CERM, Via L. Sacconi 6, 50019, Sesto Fiorentino, Italy. Fax: +39-055-4574253. E-mail: luchinat@cerm.unifi.it.

Marco Fragai, born in Cortona, Italy, on March 1, 1970, graduated in medicinal chemistry cum laude and obtained his Ph.D. in chemistry at the University of Florence, Italy. He did his postdoctoral at the Department of Chemistry until 2005 and then was a researcher at the Department of Agricultural Biotechnology and the Magnetic Resonance Center (CERM) of the University of Florence. His research interests include drug design and applications of NMR techniques in drug discovery.

Claudio Luchinat, born in Florence, Italy, on February 15, 1952, obtained his doctor in chemistry cum laude at the University of Florence, was a postdoctor and researcher at the University of Florence, and was a full Professor of Chemistry at the University of Bologna (1986−1996) and Florence (1996−) at the Department of Agricultural Biotechnology and the Magnetic Resonance Center (CERM). He is a recipient of the "Raffaello Nasini" gold medal award for inorganic chemistry of the Italian Chemical Society, 1989; Federchimica Award "For an Intelligent Future", 1994; European Medal for Biological Inorganic Chemistry, 1996; and "GDRM gold medal for magnetic resonance", 2001. He is the author of more than 400 publications in bioinorganic chemistry, NMR, and structural biology and of four books.

Giacomo Parigi, born in Borgo San Lorenzo, Italy, on September 17, 1967, graduated in physics cum laude and obtained his Ph.D. in chemistry at the University of Florence, Italy. He did his postdoctoral at the Department of Chemistry of the University of Florence and was a researcher at the Department of Agricultural Biotechnology and the Magnetic Resonance Center (CERM) of the University of Florence since 1999. His research interests include nuclear and electron relaxation, paramagnetism-based effects in NMR, and bioinformatics for structure calculations. He is the coauthor of a book on "Solution NMR of Paramagnetic Molecules" with I. Bertini and C. Luchinat.

10.1021/ar050103s CCC: $33.50
Published on Web 08/15/2006

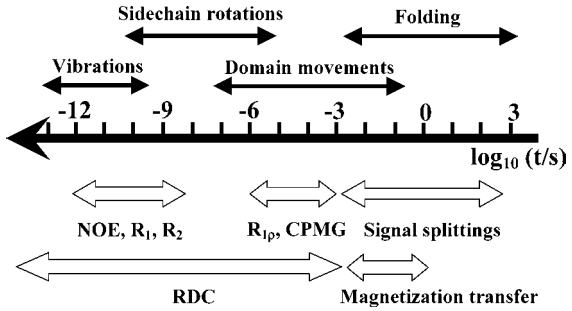

FIGURE 1. Time scales of the protein mobility and detection range of NMR techniques.

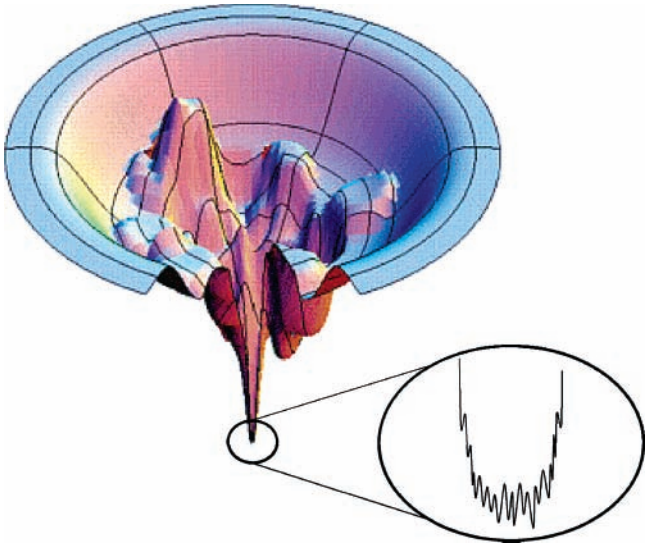

FIGURE 2. Folding funnel.

number of freely rotatable bonds. It is however customary to draw a cartoon, often called the *folding funnel* or *energy landscape*[16] (Figure 2), where the degrees of freedom on which the energy of the protein depends are reduced to two and on which possible folding trajectories may be depicted. Because we are interested in the width of the conformational space without reference to trajectories, our representation of the bottom of the funnel has only one dimension. This dimension, defined as the fourth dimension of the four-dimensional protein structure, is a 1D representation of the conformational space.

No protein can be considered rigid, because in all cases, local fluctuations on nano−picosecond time scales occur.[7] These movements can be monitored through relaxation rate studies, and an order parameter S^2 can be obtained to quantify the extent of single local motions. S^2 values larger than 0.85 are regularly observed in well-folded "rigid" proteins. We can say that, if only these fast motions are present, the width of the fourth dimension is small (Figure 3A). Other motions characterizing conformational equilibria may be present, and these may be in the nano−millisecond time scale. They usually involve collective motions of several atoms.[4,7,8] Interestingly, they are also often accompanied by smaller values of S^2, pointing to the concomitant presence of motions in faster time scales. These movements can allow the protein either to switch between two different equilibrium states (Figure 3B) or

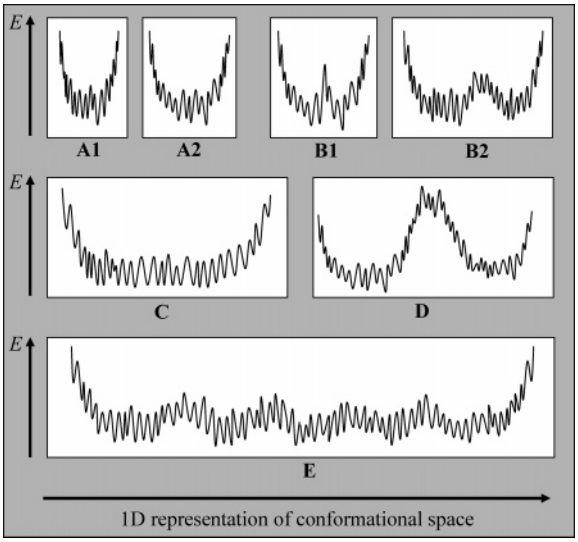

FIGURE 3. Energy profile as a function of the 1D representation of conformational space.

to move almost freely in a wide range of conformations (Figure 3C). Finally, some proteins can assume very different conformations, involving the relative movements of extended protein regions on even slower time scales, which can result in equilibria among two (Figure 3D) or a variety of (Figure 3E) different conformations.

Copper-Thionein: Metal Exchange with Minimal Conformational Width. Yeast copper-thionein (CuMT) is a small cysteine-rich protein with high affinity for copper(I) ions. MT can bind 6−8 copper(I) ions, with Cu_7MT being the most representative species. The protein folds only in the presence of copper(I) ions. The role of MT is, among others, that of a depository for copper transfer into apocopper proteins and apocopper chaperones, implying the ability to quickly bind and release copper when required. Crystallization attempts have always failed, while the solution NMR structures of M_7MT ($M = Ag^{I}$ [17] and Cu^{I} [17])[18] could be solved. The topology of the metal−cysteine binding network in Ag_7MT could be obtained by exploiting the magnetic coupling between protein nuclei and silver nuclei,[17] while this was impossible for Cu_7MT. Unfortunately, the two structures are similar but not identical,[18] indicating that Ag_7MT is not a perfect model for Cu_7MT.

A high-resolution NMR structure of Cu_7MT could be obtained only for residues 5−40, with a backbone root-mean-square deviation (rmsd) of 0.32 Å (Figure 4), while the 4 N- and 13 C-terminal residues were disordered.[18] Therefore, the central metal-bound polypeptide region has a very small fourth dimension width. The solution structure of the truncated 5−40 residues Cu_7MT was then shown to be identical to that of the holoprotein.[19] Prompted by these observations, crystallization of the truncated form was attempted and immediately achieved.[20]

Surprisingly, the crystal structure showed the presence of *eight* copper(I) ions. The structure was virtually identical to the NMR structure except for the orientation of one cysteine (inset of Figure 4), which is incompatible with copper binding in solution but is posed to coordinate the

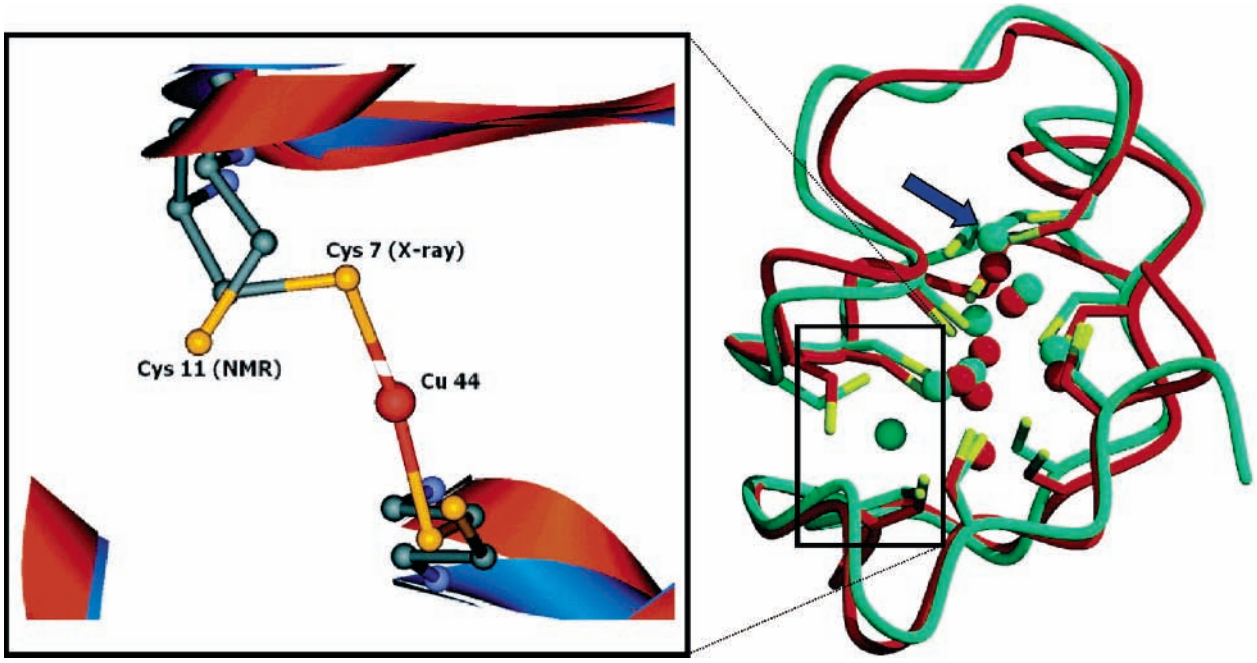

FIGURE 4. Cu_8-MT solid-state (green) and Cu_7-MT NMR (red) structures. Copper ions and cysteine side chains are indicated. The different orientation of one cysteine, which binds one additional copper in the X-ray structure, is highlighted. The arrow indicates another possibly labile copper ion. Adapted from ref 20.

eighth copper ion in the X-ray structure.[20] Apparently, crystals containing Cu_8MT were formed from a solution of Cu_7MT. Cu_6MT molecules are then left in solution, possibly lacking another copper ion, located at the other side of the cluster. These two more labile copper(I) ions may be the ones transferred fast to copper chaperones *in vivo*. It is surprising that, although the folding of MT is totally dependent upon copper(I) binding, the last (or the last two) copper(I) ions are taken up with such minimal structural rearrangement. Figure 3B1 depicts the very small width of the functional fourth dimension of the core part of CuMT, at least as far as the uptake−release of the eighth copper(I) ion is concerned. The small barrier separating the two minima is essentially relative to the local rearrangement of a cysteine side chain. On the other hand, the fourth dimension is large if the 4 N- and 13 C-terminal residues are considered. However, there is no evidence that these residues have a functional role. Remarkably, neither NMR nor X-ray alone could have provided this exhaustive picture of CuMT.

Copper Exchange between Atx1 and Ccc2a: Donor and Acceptor Have Different Conformational Widths. Atx1 is a copper-trafficking protein that can directly and reversibly donate a copper(I) ion to the first soluble domain of Ccc2 ATPase (Ccc2a).[21] In the adduct between CuAtx1 and apoCcc2a, a copper-bridged intermediate is formed (Figure 5).[22] In Atx1, the two metal-binding cysteines move from buried in the copper(I)-loaded protein to solvent-exposed after copper release. Therefore, the fourth structural dimension is of the type reported in Figure 3B2. Conversely, the structure of Ccc2a remains almost invariant upon copper(I) coordination, indicating a more pre-organized metal-binding site in apoCcc2a than in apoAtx1 and a fourth dimension more similar to that

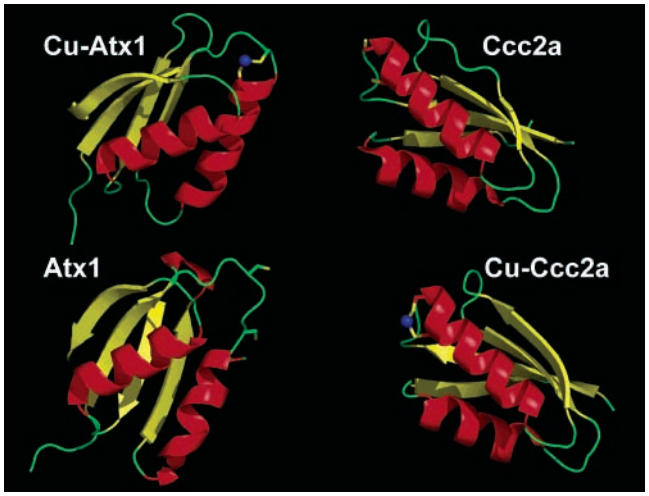

FIGURE 5. Atx and Ccc2a exchanging a copper(I) ion.

of MT (Figure 3B1). The apoproteins are much more mobile than the copper(I)-bound proteins, with Atx1 showing a larger conformational variability than Ccc2a. It would be tempting to speculate that the larger width of the fourth dimension in apoAtx1 provides an overall gain in entropy, thus helping copper(I) to pass from Atx1 to Ccc2a.

Cytochromes: What a Tiny Electron Can Do. Cytochromes are well-folded, compact electron-transfer heme proteins accessing a diamagnetic iron(II) state and a paramagnetic $S = {}^1/_2$ iron(III) state. NMR studies on iron(III) cytochromes are successfully performed by taking advantage of the additional structural information provided by paramagnetism-based restraints.[23] The NMR structures show small but significant differences between

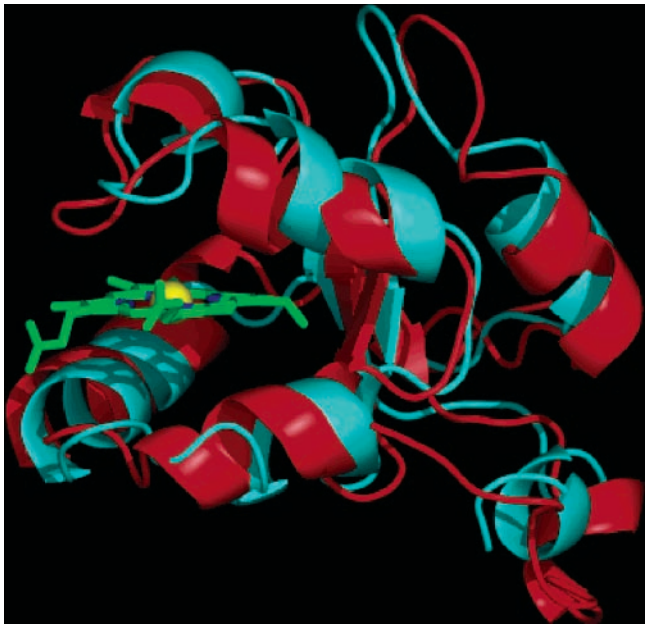

FIGURE 6. Structure of cytochrome b_5 in the oxidized (red) and reduced (cyan) forms.

the two states (Figure 6).[24,25] Reduced cytochrome b_5 is another good example of a protein sampling a small conformational width, over a fast time scale, around a well-defined equilibrium structure (Figure 3A1). However, the oxidized protein shows a marked increase in mobility in the nano−picosecond time scale, as indicated by an overall decrease in the S^2 values (Figure 7).[26,27] Off-resonance $R_{1\rho}$ experiments show that conformational exchange processes in the milli−microsecond time scale are operative in the oxidized form.[28] The majority of residues showing conformational exchange belong to helices forming the heme-binding pocket. The latter thus results to be quite flexible.

Similarly, larger mobility was found in the oxidized form with respect to the reduced form of cytochrome *c*, as shown by the smaller S^2 values and the presence of exchange processes in the milli−microsecond time scale detected with off-resonance $R_{1\rho}$ experiments and ^{1}H-^{15}N HSQC spectra in D_2O.[25] Careful inspection of the X-ray structures[29] also shows somewhat higher temperature factors in the oxidized protein.

It can be concluded that the fourth structural dimension of cytochromes increases sizably upon passing from the reduced (Figure 3A1) to the oxidized (Figure 3A2) form. It is surprising that one electron less, in a protein of 10 000 Da, can produce such large effects. However, the coordination properties of low-spin iron(III), as opposed to iron(II), are sizably different (e.g., coordination of the axial methionine in cytochrome *c* is much weaker in the oxidized form[25]). This redox-dependent flexibility in heme proteins may be not only important for molecular recognition of biological partners but also for controlling the reduction potential.[24] Finally, it strikes the imagination to think that the thermodynamic stability is so different between the two redox states that folding of the denatured oxidized cytochrome *c* can be triggered by the addition of a tiny electron![30]

A Wider Fourth Dimension in the Family of Matrix Metalloproteinases (MMPs). MMPs are extracellular proteases involved in tissue remodelling and cell signalling[31,32] and are actively studied as potential drug targets. The catalytic site is constituted by the zinc-binding region, the S1′ pocket, and the substrate-binding groove (Figure 8) and is able to bind a variety of different inhibitors. This ability may be at least in part related to a relatively large flexibility, which allows the protein to sample different conformations and thus accommodate different ligands. Therefore, it is expected that the fourth dimension is sizable in these proteins (Figure 3C).

The width of the fourth dimension of MMPs was studied by comparing several X-ray and NMR protein structures.[33] A comparison of the rmsd per residue in NMR structure families of several MMPs shows that disorder is present in the same loop regions of different proteins (Figure 9). Indeed, the loop regions found disordered in solution show different conformations in the X-ray structures of MMP-12 crystallized with three different inhibitors. The rmsd in the loop forming the S1′ cavity is as high as 3 Å. Conformational heterogeneity is confirmed by X-ray structures of other MMPs, where often some residues in this loop are missing.[33] High rmsd values in other regions indicate that MMP-12 displays conformational heterogeneity throughout the whole structure.

Several NMR techniques were applied (Figure 1) to investigate mobility in MMP-12 on the different time scales. The decrease in nuclear Overhauser effect (NOE) intensity systematically observed in some loops, in good agreement with the X-ray thermal factors, indicates mobility in the nano−picosecond time scale. ^{1}H-^{15}N relaxation, $R_{1\rho}$, and Carr−Purcell−Meiboom−Gill (CPMG) measurements, able to monitor motions on the milli−microsecond time scales, indicated that several residues were affected also by such motions. Residual dipolar couplings (rdc) provided information on the mobility of all time scales faster than or on the order of milliseconds.[1] Several measured rdc are smaller than the values calculated according to available MMP-12 structures, as the result of conformational averaging, in particular at the extremities of the loop forming the S1′ cavity and several other loops. This suggests a large amplitude of loop motions. Finally, the presence of resonance splittings in the ^{1}H-^{15}N HSQC spectra, clearly observed for residues in several loops, indicates local conformational heterogeneity with time scales on the order or longer than milliseconds.

In summary, several protein regions undergo relatively wide and collective motions. MMPs are thus a good example of the interplay among different motions and the resulting complexity of the fourth dimension. It appears that large movements of loops on the millisecond or longer time scale are always accompanied by more localized movements on the microsecond time scale. Of course, faster local movements on the nano−picosecond time scale are universally present.

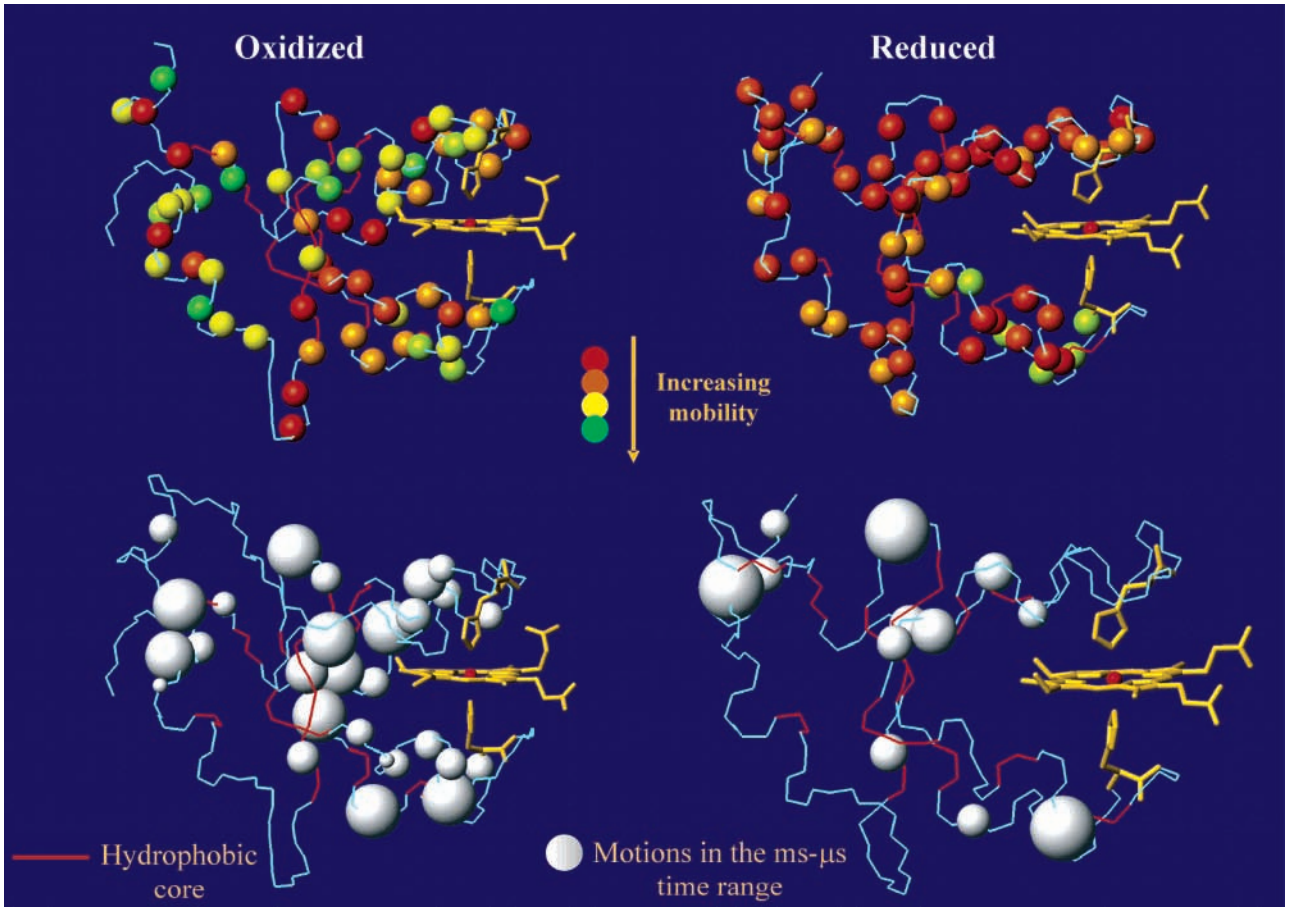

FIGURE 7. Internal mobility in cytochrome b_5 in the oxidized and reduced forms, in the nano−picosecond range (left) and in the milli−microsecond range (right). The sphere radii are proportional to the exchange rates.

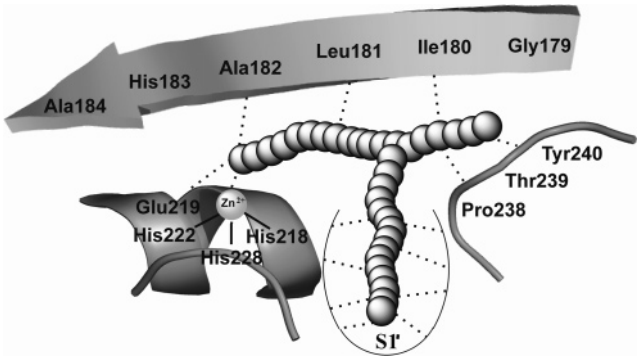

FIGURE 8. General substrate-binding mode in the catalytic site of MMPs.

Signalling by EF-Hand Proteins Needs a Wide Fourth Dimension

The EF-hand motif is a helix−loop−helix motif that has the ability to bind one calcium ion. In doing so, the relative orientation of the two helices changes, passing from a roughly antiparallel arrangement (closed or parallel bundle form) to an almost perpendicular arrangement (open or orthogonal bundle form).[34,35] Two EF-hand motifs connected by a short linker constitute a EF-hand domain, which is the functional unit recognized as the universal calcium signal transducer (Figure 10). Its evolutionary success resides in calcium-binding cooperativity, enhancing the opening of the whole domain. The calcium form exposes a large part of the hydrophobic core, and the resulting hydrophobic cavity is a very good binder for amphypatic α-helical motifs present in a variety of target proteins. An increase in intracellular calcium concentration triggers the EF-hand domains into their open forms, which in turn bind target proteins and trigger biological responses.

Calmodulin (CaM) is the perfect machine for this task. It is constituted by *two* EF-hand domains, connected by a linker. The two domains arise from gene duplication and are very similar to one another. Therefore, target binding is enhanced, because the target peptide can be clamped between the two domains (Figure 11). Given the amplitude and functional relevance of the associated conformational changes, exploring in detail the fourth structural dimension of CaM and EF proteins in general is a necessary and fascinating task.

Fourth Dimension of Individual EF-Hand Domains. The two CaM domains are not exactly alike. ^{15}N relaxation rates and ^{1}H and ^{15}N NMR spectra of apoCaM show that the N-terminal domain adopts a static antiparallel helical conformation,[36,37] while the C-terminal domain undergoes dynamic exchange between an antiparallel (~95% of the molecules) and one or more not parallel helical arrangements (Figure 12).[38,39] Indeed, the C-terminal domain of apoCaM obtained in nearly identical conditions adopts

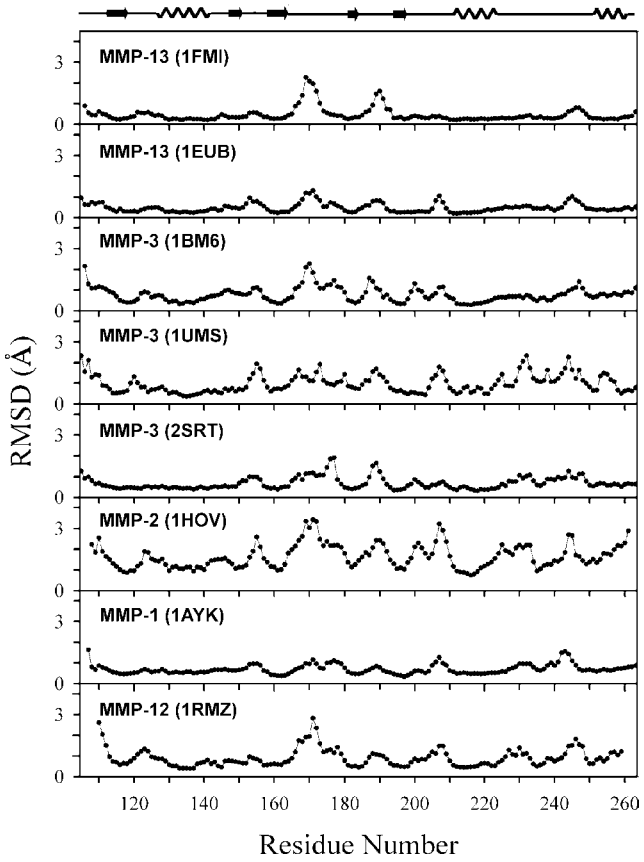

FIGURE 9. rmsd per residue for the NMR structure families of various MMPs (adapted from ref 33).

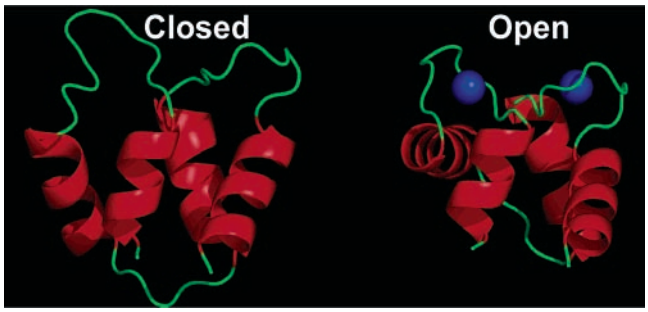

FIGURE 10. EF-hand motifs in the closed and open forms in the presence of calcium ions.

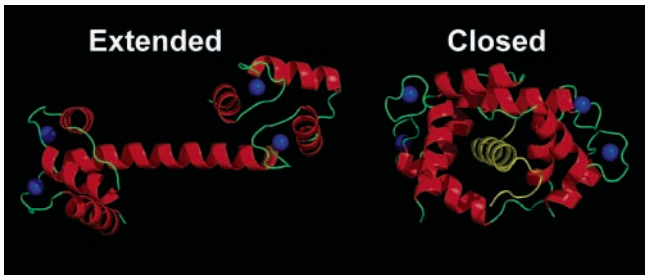

FIGURE 11. Extended structure of free CaM and closed structure in peptide adducts.

substantially different conformations,[37,40] despite the order parameter for secondary-structure elements is as expected for well-folded proteins ($S^2 \sim 0.85$).[38] Furthermore, the solution structure of calcium(II)-loaded CaM indicates that

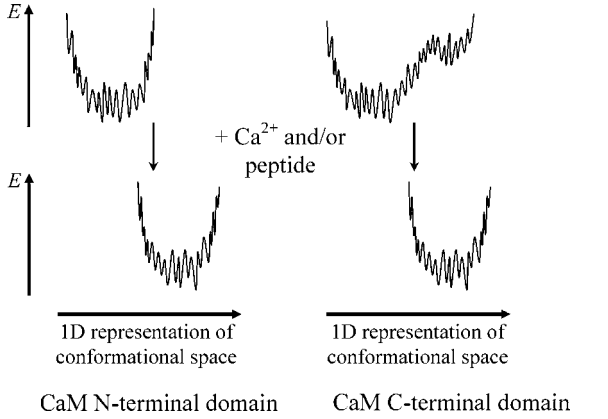

FIGURE 12. N- and C-terminal domains of the CaM switch from an (essentially) closed to an open conformation upon calcium and/or peptide binding.

the N-terminal domain is considerably less open with respect to the X-ray structure.[36] Different from the apoCaM, both the N- and C-terminal domains of calcium(II)-loaded CaM exist only in the open (or semi-open) state.[36] A dynamic equilibrium involving conformations with a partially exposed hydrophobic core thus provides CaM with the ability to interact with its targets in the absence of excess calcium(II).[41] Target binding then moves the equilibrium toward the open state.[42] All of these findings indicate that EF-hand domains have a remarkably large fourth dimension, independent of the presence of calcium(II), and that the latter simply "drives" the protein from one conformational energy minimum to another. This interpretation fits recent views on allosteric regulation.[9,11]

Fourth Dimension of CaM. The definition of the relative position of the two CaM domains is a formidable task. Early X-ray structures of calcium(II)-loaded CaM suggested that the last helix of the N-terminal domain, the first helix of the C-terminal domain, and the interdomain linker constitute a long continuous helix. Such conformation is inconsistent with NMR data in solution, which show high mobility of residues 78−81 in the interdomain linker, indicating that the helical structure in such a region is disrupted.[43,44] Disorder in the interdomain linker was subsequently confirmed also in the solid state.[45] Remarkably, a crystal structure has recently appeared in which the two domains touch each other.[46] Conversely, one X-ray structure of apoCaM also reports the N- and C-terminal domains to interact,[40] whereas the solution structures indicate the absence of stable contacts between the two domains.[37] It appears as though X-ray structures only provide snapshots of either closed, compact, or open, fully elongated forms.

The relative conformational freedom of the two CaM domains was explored using paramagnetism-based NMR restraints.[47] Pseudocontact shifts and rdc were obtained for a suitably designed CaM mutant,[48] where terbium(III) or thulium(III) were selectively substituted at the second binding site, with calcium(II) in the other three sites. If there were no relative motions, the spreading of the lanthanide-induced rdc should be approximately the same

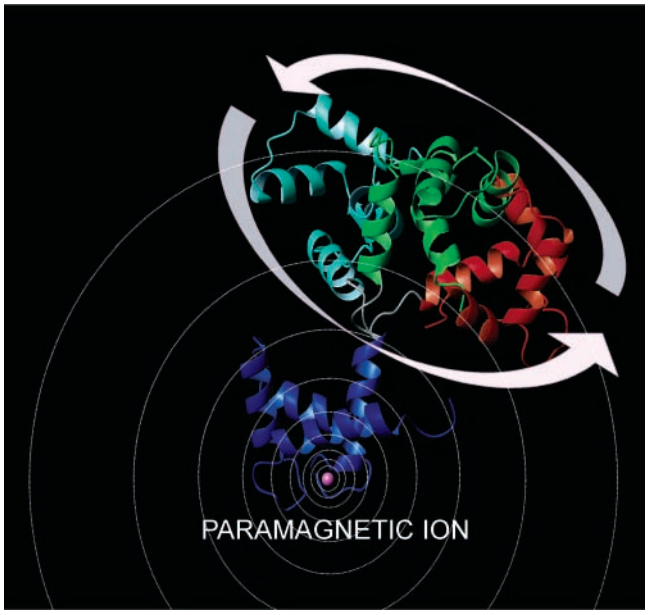

FIGURE 13. C-Terminal domain of CaM moves within a wide elliptical cone about the axis defined by the last helix of the N-terminal domain. Three possible conformations are shown.

in both domains, and their analysis would easily provide the relative orientation of the two domains. However, the rdc spreading in the C-terminal domain was found to vary between 5 and 15% of that of the N-terminal domain,[47] showing that the relative motions are very large. However, not all sterically allowed conformations are equally populated: with respect to the N-terminal domain, the C-terminal domain was found to preferentially reside in a region of space roughly inscribed in a wide elliptical cone[47] (Figure 13). Apparently, CaM possesses a particularly wide fourth dimension, being able to sample a large range of very different conformations, as schematically depicted in Figure 3E. X-ray structures provide snapshots of conformations that may not even be the most populated ones.

Other EF-Hand Proteins: Variations on the Theme. Calbindin D_{9k} (Cb) is a single EF-hand domain protein. Its structure is known both in the apo and in the dicalcium form (Figure 14).[49] A solution structure of monolanthanide-substituted Cb with a very low backbone rmsd (0.25 Å) was obtained using paramagnetism-based NMR restraints.[50] Very small changes in the conformation of the first EF-hand motif occur upon calcium(II) binding,[42] and somewhat larger but still minor changes occur in the second EF-hand motif.[51] Relaxation data indicate that the flexibility of Cb is largely reduced upon calcium(II) binding, particularly in the loop of the second EF-hand motif.[52] The resulting reduction in nano−picosecond time scale dynamics correlates with the loss of conformational entropy and affects substantially the calcium-binding affinity.[5,53,54] The width of the fourth dimension in calbindin is thus small, e.g., as in Figure 3A1 for Ca_2Cb and as in Figure 3A2 for apoCb.

EF-hand proteins such as Cb function as calcium buffers and carriers. Conformational changes are avoided in this case, because these would lead to a reduction in calcium(II) affinity. Cb avoids conformational changes through mutations in one of the loops, which uncouple calcium binding and domain opening. The inequivalence of the two EF-hand motifs is illustrated by, e.g., the selective lanthanide substitution to only one site (Figure 14). Other calcium buffer EF-hand proteins like α-parvalbumin (PV) and *β*-parvalbumin (OM) avoid opening through a different mechanism. They originate from a CaM ancestor lacking the first of the four EF-hand motifs. The second motif then lost its calcium-binding ability, while the C-terminal domain remained functional. NMR[55,56] and X-ray[57,58] structures of PV and OM show that the first EF-hand motif resembles a peptide permanently bound to the open form of the C-terminal domain (Figure 15). In this way, apoPV and apoOM are already in a peptide-bound form and ready to bind two calcium ions, therefore,

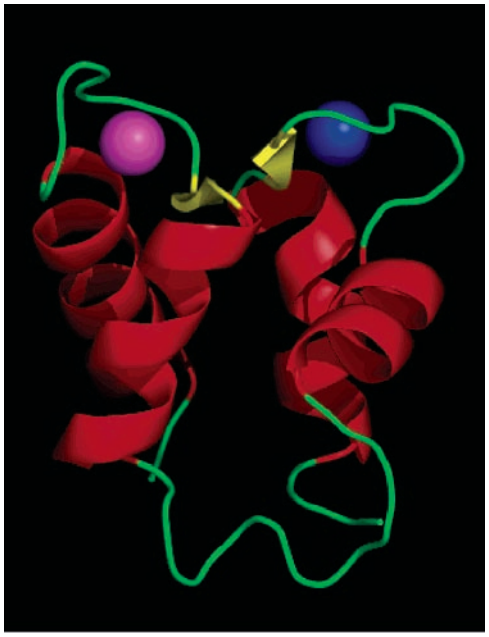

FIGURE 14. Structure of Cb. The calcium ion in violet is located in the modified EF-hand motif, and the one in blue can be selectively substituted by lanthanides.[50]

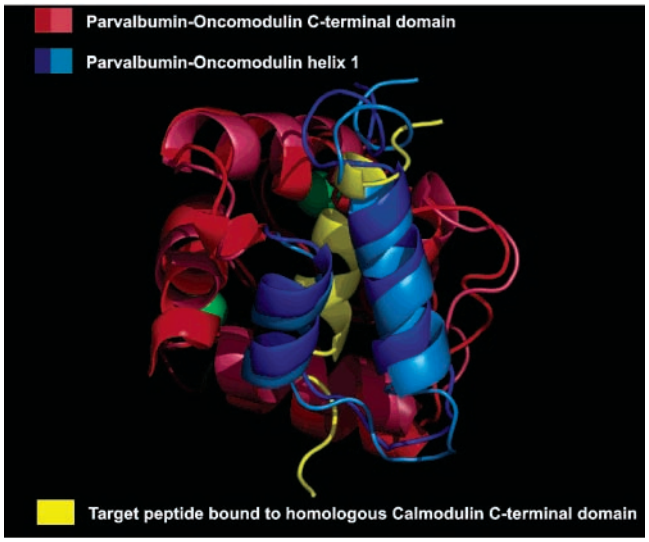

FIGURE 15. Superimposed structures of PV and OM.

with high affinity. Figure 3A is again adequate to describe the situation of calcium-bound PV and OM.

EF-hand domains thus span a large variety of fourth dimension widths. We have recently found a CaM-like protein with a N-terminal domain having the normal four-helices secondary structure, little or no tertiary structure, and erratic calcium-binding properties.[59]

Conclusions and Perspectives

Protein conformational heterogeneity can be viewed as a fourth structural dimension. In some cases (e.g., CaM), the latter can be quite large. Even in proteins with a smaller fourth dimension, conformational heterogeneity may play important roles. For instance, in catalytic enzymes, it allows binding sites to adapt to a more or less large variety of substrates (and/or inhibitors).[1−3] The knowledge of the whole set of allowed conformations rather than of a single averaged conformation may be fundamental for rationalizing the inhibitor-binding capability of drug targets.[5,60,61] As computational methods become more and more powerful, there are hopes that predictions of molecular mobility on times longer than nanoseconds can be obtained by molecular dynamics simulations or normal-mode approaches.[62,63]

In this Account, we have attempted to stress the importance of conformational heterogeneity of proteins, with examples taken from the world of metalloproteins. Upon passing from the genomic to the proteomic era, we need to have a clear mental representation of the main actors, the proteins, not as static but as dynamic objects. The proteome gives rise to the interactome, and dynamics is at the core of the proper understanding of protein−protein and protein−biomolecule interactions. We foresee that the increasing awareness, on the side of structural biologists, of the richness of functional information contained in the conformational heterogeneity of a protein will lead us not to consider a protein structural investigation complete until data on the width of this fourth structural dimension is provided.

We thank Ivano Bertini for his precious comments and suggestions. Support by the European Commission (contracts QLG2-CT-2002-00988 and LSHG-CT-2004-512052), MIUR-PRIN (contract 2005039878), and Ente Cassa di Risparmio, Florence, Italy, is acknowledged.

References

(1) Wang, L. C.; Pang, Y. X.; Holder, T.; Brender, J. R.; Kurochkin, A. V.; Zuiderweg, E. R. P. Functional Dynamics in the Active Site of the Ribonuclease Binase. *Proc. Natl. Acad. Sci. U.S.A.* 2001, *98*, 7684−7689.

(2) (a) Eisenmesser, E. Z.; Bosco, D. A.; Akke, M.; Kern, D. Enzyme Dynamics During Catalysis. *Science* **2002**, *295*, 1520−1523. (b) Eisenmesser, E. Z.; Millet, O.; Labeikovsky, W.; Korzhnev, D. M.; Wolf-Watz, M.; Bosco, D. A.; Skalicky, J. J.; Kay, L. E.; Kern, D. Intrinsic Dynamics of an Enzyme Underlies Catalysis. *Nature* **2005**, *438*, 117−121.

(3) Lindorff-Larsen, K.; Best, R. B.; DePristo, M. A.; Dobson, C. M.; Vendruscolo, M. Simultaneous Determination of Protein Structure and Dynamics. *Nature* **2005**, *433*, 128−132.

(4) Ishima, R.; Torchia, D. A. Protein Dynamics from NMR. *Nat. Struct. Biol.* **2000**, *7*, 740−743.

(5) Jarymowycz, V. A.; Stone, M. J. Fast Time Scale Dynamics of Protein Backbones: NMR Relaxation Methods, Applications, and Functional Consequences. *Chem. Rev.* **2006**, *106*, 1624−1671.

(6) Mulder, F. A. A.; Mittermaier, A.; Hon, B.; Dahlquist, F. W.; Kay, L. E. Studying Excited States of Proteins by NMR Spectroscopy. *Nat. Struct. Biol.* **2001**, *8*, 932−935.

(7) Kay, L. E. Protein Dynamics from NMR. *Nat. Struct. Biol.* **1998**, *5*, 513−517.

(8) Huang, Y. J.; Montelione GT Structural Biology: Proteins Flex to Function. *Nature* **2005**, *438*, 36−37.

(9) Volkman, B. F.; Lipson, D.; Wemmer, D. E.; Kern, D. Two-State Allosteric Behavior in a Single-Domain Signaling Protein. *Science* **2001**, *291*, 2429−2433.

(10) Valentine, E. R.; Palmer, A. G. Microsecond-to-Millisecond Conformational Dynamics Demarcate the GluR2 Glutamate Receptor Bound to Agonists Glutamate, Quisqualate, and AMPA. *Biochemistry* **2005**, *44*, 3410−3417.

(11) Kern, D.; Zuiderweg, E. R. The Role of Dynamics in Allosteric Regulation. *Curr. Opin. Struct. Biol.* **2003**, *13*, 748−757.

(12) Fischer, M. W. F.; Zeng, L.; Majumdar, A.; Zuiderweg, E. R. P. Characterizing Semilocal Motions in Proteins by NMR Relaxation Studies. *Proc. Natl. Acad. Sci. U.S.A.* **1998**, *95*, 8016−8019.

(13) Brüschweiler, R. New Approaches to the Dynamic Interpretation and Prediction of NMR Relaxation Data from Proteins. *Curr. Opin. Struct. Biol.* **2003**, *13*, 175−183.

(14) (a) Mittermaier, A.; Kay, L. E. Review—New Tools Provide New Insights in NMR Studies of Protein Dynamics. *Science* **2006**, *312*, 224−228. (b) Brath, U.; Akke, M.; Yang, D. W.; Kay, L. E.; Mulder, F. A. A. Functional Dynamics of Human FKBP12 Revealed by Methyl C-13 Rotating Frame Relaxation Dispersion NMR Spectroscopy. *J. Am. Chem. Soc.* **2006**, *128*, 5718−5727.

(15) Christodoulou, J.; Larsson, G.; Fucini, P.; Connell, S. R.; Pertinhez, T. A.; Hanson, C. L.; Redfield, C.; Nierhaus, K. H.; Robinson, C. V.; Schleucher, J.; Dobson, C. M. Heteronuclear NMR Investigation of Dynamic Regions of Intact *Escherichia coli* Ribosomes. *Proc. Natl. Acad. Sci. U.S.A.* **2004**, *101*, 10949−10954.

(16) (a) Dobson, C. M. Protein Folding and Misfolding. *Nature* **2003**, *426*, 884−890. (b) Dill, K. A.; Chan, H. S. From Levinthal to Pathways to Funnels. *Nat. Struct. Biol.* **1997**, *4*, 10−19.

(17) Peterson, C. W.; Narula, S. S.; Armitage, I. M. 3D Solution Structure of Copper and Silver-Substituted Yeast Metallothioneins. *FEBS Lett.* **1996**, *379*, 85−93.

(18) Bertini, I.; Hartmann, H. J.; Klein, T.; Liu, G.; Luchinat, C.; Weser, U. High Resolution Solution Structure of the Protein Part of Cu_7 Metallothionein. *Eur. J. Biochem.* **2000**, *267*, 1008−1018.

(19) Luchinat, C.; Dolderer, B.; Del Bianco, C.; Echner, H.; Hartman, H.; Voelter, W.; Weser, U. The $Cu(1)_7$ Cluster in Yeast Copper Thionein Survives Major Shortening of the Polypeptide Backbone as Deduced from Electronic Absorption, Circular Dichroism, Luminescence and ^{1}H-NMR. *J. Biol. Inorg. Chem.* **2003**, *8*, 353−359.

(20) Calderone, V.; Del Bianco, C.; Dolderer, B.; Echner, H.; Hartmann, H. J.; Luchinat, C.; Mangani, S.; Weser, U. The Crystal Structure of Yeast Copper Thionein: The Solution of a Long-Lasting Enigma. *Proc. Natl. Acad. Sci. U.S.A.* **2005**, *102*, 51−56.

(21) Huffman, D. L.; O'Halloran, T. V. Energetics of Copper Trafficking Between the Atx1 Metallochaperone and the Intracellular Copper-Transporter, Ccc2. *J. Biol. Chem.* **2000**, *275*, 18611−18614.

(22) Banci, L.; Bertini, I.; Cantini, F.; Felli, I. C.; Gonnelli, L.; Hadjiliadis, N.; Pierattelli, R.; Rosato, A.; Voulgaris, P. The Atx1−Ccc2 Complex Is a Metal-Mediated Protein−Protein Interaction. *Nat. Chem. Biol.* **2006**, *2*, 367−368.

(23) Bertini, I.; Luchinat, C.; Parigi, G. Magnetic Susceptibility in Paramagnetic NMR. *Progr. NMR Spectrosc.* **2002**, *40*, 249−273.

(24) Arnesano, F.; Banci, L.; Bertini, I.; Felli, I. C.; Koulougliotis, D. Solution Structure of the B Form of Oxidized Rat Microsomal Cytochrome b_5 and Backbone Dynamics Via ^{15}N Rotating Frame NMR Relaxation Measurements: Biological Implications. *Eur. J. Biochem.* **1999**, *260*, 347−354.

(25) Barker, P. B.; Bertini, I.; Del Conte, R.; Ferguson, S. J.; Hajieva, P.; Tomlinson, E. J.; Turano, P.; Viezzoli, M. S. A Further Clue to Understanding the Mobility of Mitochondrial Yeast Cytocrome *c*: A ^{15}N T1p Investigation of the Oxidized and Reduced Species. *Eur. J. Biochem.* **2001**, *268*, 4468−4476.

(26) Dangi, B.; Blankman, J.; Miller, C. J.; Volkman, B. F.; Guiles, R. D. Contribution of Backbone Dynamics to Entropy Changes Occurring on Oxidation of Cytochrome b_5; Can Redox Linked Changes in Hydrogen Bond Networks Modulate Reduction Potentials? *J. Phys. Chem. B* **1998**, *102*, 8201−8208.

(27) Arnesano, F.; Banci, L.; Bertini, I.; Koulougliotis, D.; Monti, A. Monitoring Mobility in the Early Steps of Unfolding: The Case of Oxidized Cytochrome b_5 in the Presence of 2 M Guanidinium Chloride. *Biochemistry* **2000**, *39*, 7117−7130.
(28) Banci, L.; Bertini, I.; Cavazza, C.; Felli, I. C.; Koulougliotis, D. Probing the Backbone Dynamics of Oxidized and Reduced Rat Microsomal Cytochrome b_5 Via ^{15}N Rotating Frame NMR Relaxation Measurements: Biological Implications. *Biochemistry* **1998**, *37*, 12320−12330.
(29) Berghuis, A. M.; Brayer, G. D. Oxidation State-Dependent Conformational Changes in Cytochrome *c*. *J. Mol. Biol.* **1992**, *223*, 959−976.
(30) Pascher, T.; Chesick, J. P.; Winkler, J. R.; Gray, H. B. Protein Folding Triggered by Electron Transfer. *Science* **1996**, *271*, 1558−1560.
(31) Maskos, K.; Bode, W. Structural Basis of Matrix Metalloproteinases and Tissue Inhibitors of Metalloproteinases. *Mol. Biotechnol.* **2003**, *25*, 241−266.
(32) Boire, A.; Covic, L.; Agarwal, A.; Jacques, S.; Sherifl, S.; Kuliopulos, A. PAR1 Is a Matrix Metalloprotease-1 Receptor That Promotes Invasion and Tumorigenesis of Breast Cancer Cells. *Cell* **2005**, *120*, 303−313.
(33) Bertini, I.; Calderone, V.; Cosenza, M.; Fragai, M.; Lee, Y.-M.; Luchinat, C.; Mangani, S.; Terni, B.; Turano, P. Conformational Variability of MMPs: Beyond a Single 3D Structure. *Proc. Natl. Acad. Sci. U.S.A.* **2005**, *102*, 5334−5339.
(34) Ikura, M. Calcium Binding and Conformational Response in EF-Hand Proteins. *Trends Biochem. Sci.* **1996**, *21*, 14−17.
(35) Babini, E.; Bertini, I.; Capozzi, F.; Luchinat, C.; Quattrone, A.; Turano, M. Principal Component Analysis of a Comprehensive Structural Database of EF-Hand Domains To Describe the Conformational Freedom within the EF-Hand Superfamily. *J. Proteome Res.* **2005**, *4*, 1961−1971.
(36) Chou, J. J.; Li, S.; Klee, C. B.; Bax, A. Solution Structure of Ca^{2+} Calmodulin Reveals Flexible Hand-Like Properties of Its Domains. *Nature Struct. Biol.* **2001**, *8*, 990−997.
(37) Zhang, M.; Tanaka, T.; Ikura, M. Calcium-Induced Conformational Transition Revealed by the Solution Structure of Apo Calmodulin. *Nat. Struct. Biol.* **1995**, *2*, 758−767.
(38) Malmendal, A.; Evenäs, J.; Forsén, S.; Akke, M. Structural Dynamics in the C-Terminal Domain of Calmodulin at Low Calcium Levels. *J. Mol. Biol.* **1999**, *293*, 883−899.
(39) Evenäs, J.; Malmendal, A.; Akke, M. Dynamics of the Transition Between Open and Closed Conformations in a Calmodulin C-Terminal Domain Mutant. *Structure* **2001**, *9*, 185−195.
(40) Schumacher, M. A.; Crum, M.; Miller, M. C. Crystal Structures of Apocalmodulin and Apocalmodulin/SK Potassium Channel Gating Domain Complex. *Structure* **2004**, *12*, 849−860.
(41) Swindells, M. B.; Ikura, M. Pre-Formation of the Semi-Open Conformation by the Apo-Calmodulin C-Terminal Domain and Implications Binding IQ-Motifs. *Nat. Struct. Biol.* **1996**, *3*, 501−504.
(42) Bhattacharya, S.; Bunick, C. G.; Chazin, W. J. Target Selectivity in EF-Hand Calcium Binding Proteins. *Biochim. Biophys. Acta* **2004**, *1742*, 69−79.
(43) Barbato, G.; Ikura, M.; Kay, L. E.; Pastor, R. W.; Bax, A. Backbone Dynamics of Calmodulin Studied by ^{15}N Relaxation Using Inverse Detected Two-Dimensional NMR Spectroscopy; the Central Helix Is Flexible. *Biochemistry* **1992**, *31*, 5269−5278.
(44) Baber, J. L.; Szabo, A.; Tjandra, N. Analysis of Slow Interdomain Motion of Macromolecules Using NMR Relaxation Data. *J. Am. Chem. Soc.* **2001**, *123*, 3953−3959.
(45) Wilson, M. A.; Brunger, A. T. The 1.0 Å Crystal Structure of Ca^{2+}-Bound Calmodulin: An Analysis of Disorder and Implications for Functionally Relevant Plasticity. *J. Mol. Biol.* **2000**, *301*, 1237−1256.
(46) Fallon, J. L.; Quiocho, F. A. A Closed Compact Structure of Native Ca^{2+}-Calmodulin. *Structure* **2003**, *11*, 1303−1307.
(47) Bertini, I.; Del Bianco, C.; Gelis, I.; Katsaros, N.; Luchinat, C.; Parigi, G.; Peana, M.; Provenzani, A.; Zoroddu, M. A. Experimentally Exploring the Conformational Space Sampled by Domain Reorientation in Calmodulin. *Proc. Natl. Acad. Sci. U.S.A.* **2004**, *101*, 6841−6846.
(48) Bertini, I.; Gelis, I.; Katsaros, N.; Luchinat, C.; Provenzani, A. Tuning the Affinity for Lanthanides of Calcium Binding Proteins. *Biochemistry* **2003**, *42*, 8011−8021.
(49) Svensson, L. A.; Thulin, E.; Forsén, S. Proline Cis−Trans Isomers in Calbindin D_{9k} Observed by X-Ray Crystallography. *J. Mol. Biol.* **1992**, *223*, 601−606.
(50) Bertini, I.; Donaire, A.; Jiménez, B.; Luchinat, C.; Parigi, G.; Piccioli, M.; Poggi, L. Paramagnetism-Based versus Classical Constraints: An Analysis of the Solution Structure of Ca Ln Calbindin D_{9k}. *J. Biomol. NMR* **2001**, *21*, 85−98.
(51) Akke, M.; Forsén, S.; Chazin, W. J. Solution Structure of $(Cd^{2+})_1$-Calbindin D_{9k} Reveals Details of the Stepwise Structural Changes along the Apo → $(Ca^{2+})_1^{II}$ → $(Ca^{2+})_2^{I,II}$ Binding Pathway. *J. Mol. Biol.* **1995**, *252*, 102−121.
(52) Akke, M.; Skelton, N. J.; Kördel, J.; Palmer, A. G., III; Chazin, W. J. Effects of Ion Binding on the Backbone Dynamics of Calbindin D_{9k} Determined by ^{15}N NMR Relaxation. *Biochemistry* **1993**, *32*, 9832−9844.
(53) Akke, M.; Brüschweiler, R.; Palmer, A. G., III NMR Order Parameters and Free Energy: An Analytical Approach and Its Application to Cooperative Ca^{2+} Binding by Calbindin D_{9k}. *J. Am. Chem. Soc.* **1993**, *115*, 9832−9833.
(54) Yang, D. W.; Kay, L. E. Contributions to Conformational Entropy Arising from Bond Vector Fluctuations Measured from NMR-Derived Order Parameters: Application to Protein Folding. *J. Mol. Biol.* **1996**, *263*, 369−382.
(55) Babini, E.; Bertini, I.; Capozzi, F.; Del Bianco, C.; Holleder, D.; Kiss, T.; Luchinat, C.; Quattrone, A. Solution Structure of Human β-Parvalbumin and Structural Comparison with Its Paralog α-Parvalbumin and with Their Rat Orthologs. *Biochemistry* **2004**, *43*, 16076−16085.
(56) Baig, I.; Bertini, I.; Del Bianco, C.; Gupta, Y. K.; Lee, Y.-M.; Luchinat, C.; Quattrone, A. Paramagnetism-Based Refinement Strategy for the Solution Structure of Human α-Parvalbumin. *Biochemistry* **2004**, *43*, 5562−5573.
(57) McPhalen, C. A.; Sielecki, A. R.; Santarsiero, B. D.; James, M. N. Refined Crystal Structure of Rat Parvalbumin, a Mammalian α-Lineage Parvalbumin, at 2.0 Å Resolution. *J. Mol. Biol.* **1994**, *235*, 718−732.
(58) Ahmed, F. R.; Rose, D. R.; Evans, S. V.; Pippy, M. E.; To, R. Refinement of Recombinant Oncomodulin at 1.30 Å Resolution. *J. Mol. Biol.* **1993**, *230*, 1216−1224.
(59) Babini, E.; Bertini, I.; Capozzi, F.; Chirivino, E.; Luchinat, C. A Structural and Dynamic Characterization of the EF-Hand Protein CLSP. *Structure* **2006**, *14*, 1029−1038.
(60) Bertini, I.; Fragai, M.; Giachetti, A.; Luchinat, C.; Maletta, M.; Parigi, G.; Yeo, K. J. Combining in Silico Tools and NMR Data To Validate Protein−Ligand Structural Models: Application to Matrix Metalloproteinases. *J. Med. Chem.* **2005**, *48*, 7544−7559.
(61) Teague, S. J. Implications of Protein Flexibility for Drug Discovery. *Nat. Rev. Drug Discovery* **2003**, *2*, 527−541.
(62) Shepherd, C. M.; Vogel, H. J. A Molecular Dynamics Study of Ca^{2+}-Calmodulin: Evidence of Interdomain Coupling and Structural Collapse on the Nanosecond Timescale. *Biophys. J.* **2004**, *87*, 780−791.
(63) Micheletti, C.; Carloni, P.; Maritan, A. Accurate and Efficient Description of Protein Vibrational Dynamics: Comparing Molecular Dynamics and Gaussian Models. *Proteins* **2004**, *55*, 635−645.

AR050103S